Journal of Metals, Materials and Minerals, Vol. 32, No. 3, pp. 68-74, 2022

Synthesis and antimicrobial studies of nano-copper doped carbon substrates; activated carbon, reduced graphene oxide, and carbon nanofiber

Songwuit CHANTHEE[1], Malee SANTIKUNAPORN[1,*], Jenjira JIRASANGTHONG[1], and Channarong ASASVATESANUPAP[2]

[1] Department of Chemical Engineering, Thammasat School of Engineering, Thammasat University, Phahonyothin, Pathum Thani, Khlong Luang, 12120, Thailand

[2] Department of Mechanical Engineering, Thammasat School of Engineering, Thammasat University, Phahonyothin, Pathum Thani, Khlong Luang, 12120, Thailand

***Corresponding author e-mail:** smalee@engr.tu.ac.th

Received date:
24 May 2022
Revised date
23 July 2022
Accepted date:
31 July 2022

Keywords:
Antimicrobial;
Copper;
Activated carbon;
Reduced graphene oxide;
Carbon Nanofiber

Abstract

Copper oxides (Cu_xO) have received considerable attention as a result of their biological activity. Nanoparticles (NPs) of Cu_xO attached to different substrates exhibit a wide spectrum of antimicrobial activity against bacteria and viruses, with similar properties to silver. The antimicrobial activity of Cu_xO-NPs doped on distinctive carbon materials was investigated for three carbon substrates: apricot stone activated carbon (AAC), reduced graphene oxide (rGO) and carbon nanofiber (CNF). The Cu_xO-NPs (5 wt%) doped AAC and rGO substrates were prepared by impregnation of copper nitrate followed by a thermal treatment process, while a similar weight of Cu_xO-NPs doped CNF was fabricated by electrospinning copper nitrate with polyacrylonitrile precursor, followed by carbonization. The Cu_xO species and chemical functions were characterized by X-ray diffraction and Fourier transform infrared spectroscopy, respectively. Surface morphology was measured using scanning electron microscopy. The antimicrobial activities of the substrates were evaluated by inhibition zone measurement of *Staphylococcus aureus* and *Escherichia coli*. The results demonstrated significant inhibition distances for different carbon substrates. Interestingly, Cu_xO-NPs doped over both AAC and rGO surfaces revealed clear zones against bacteria, whereas the inhibition zone was not recorded for Cu_xO-NPs doped over a CNF substrate. Various parameters such as carbon substrates, particle size, and copper oxide species were investigated.

1. Introduction

Infection from pathogens is harmful to human health and can potentially cause death [1,2]. The antimicrobial properties of nano-materials (NMs) have recently received increasing attention due to concerns about infection from microorganisms such as bacteria and viruses. However, the usage of these NMs may involve irreversible adverse effects on human health, especially carcinogenicity and genotoxicity. Most metal (oxide) nanoparticles (MNPs), such as titanium (Ti), copper (Cu), gold (Au), silver (Ag), zinc (Zn), or magnesium (Mg), not only promote the production of reactive oxygen species (ROS) but also stimulate reduction/oxidation reactions that cause cell damage [3,4]. Besides MNPs, exposure to carbon-based NMs such as carbon nanotubes, fullerenes, graphene (oxide), carbon black, carbon nanofibers (CNFs) and their derivatives, can also lead to inflammation damage of genetic materials. Furthermore, cancer formation in living organisms is initiated by the production of mutations and genome instability formation after exposure to carcinogens [5]. The degree of toxicity for these NMs is altered but can be correlated well with their structural and physical properties such as size, shape, surface modification, exposure routes, etc. [6].

To improve the antimicrobial performances of materials, MNs (Ti, Au, Ag, Zn, Cu, or Mg) with antimicrobial activity were applied to the material matrix [7-9]. Among antimicrobial metals, copper nano-particles (CuNPs) possess antifungal, antimicrobial, and antiviral properties and have been widely utilized as they are inexpensive and exhibit acceptable activity. However, several previous studies have reported that high concentrations of CuNPs had a toxic effect on many microorganisms [10-13]. Therefore, searching for a suitable substrate that can reduce the toxicity of CuNPs while effectively exhibiting antimicrobial action at low quantities of CuNPs was considered. Copper-doped high surface areas have been shown to increase bacterial reduction and inhibition zones. Antimicrobial activity investigations for different species of Cu_xO have found that they presented lower toxicity than copper in metallic form, whereas the reduction of pathogens was still observed [14]. Copper oxide nano-particles have also shown high anti-microbial performance after loading onto high specific surface area materials such as porous oxides, polymers, and carbon substrates [15,16].

Previous literature supported the premise that carbon substrates promoted the dispersion of antimicrobial metals and metal oxides [16]. Carbon substrates can be used to carry active metal nanoparticles into other materials while maintaining their antimicrobial properties. The investigation of copper oxide nanoparticle-decorated on carbon nanocomposite material has shown efficient antimicrobial and antiproliferative activities against bacteria and cancer cells [17]. However, carbon-based materials for Cu_xO nanoparticle dopants have certain disadvantages. For instance, these particles dominantly aggregate into larger sizes over the carbon surface [18], while antimicrobial activity is reduced by the uncertain morphology of activated carbon [19]. In this study, Cu_xO-NPs loaded on three different carbon substrates (activated carbon; AC, reduced graphene oxide; rGO, and CNFs) were investigated for their antibacterial activities against pathogens. The size and dispersion of the Cu_xO-NPs were also examined.

2. Experimental

As presented in Figure 1, different carbon structures were employed as substrates for copper oxide anchoring. Three carbon substrates (AAC, CAC, and rGO) were doped with copper nitrate (5 wt% based Cu metal) by impregnation method. On the other hand, the CNF substrate was doped with 5 wt% of copper nitrates by mixing into the PAN polymeric precursor prior to being electrospun to fiber form. All samples were further treated under a suitable thermal process to obtain each copper oxide doped carbon substrate, which was described in detail.

2.1 Materials

All chemicals were commercially available and used without further purification. Polyacrylonitrile (PAN) (ca. MW = 150,000) was purchased from Sigma-Aldrich. Apricot stones were supplied by Doi Kham Food Products Co., Ltd. Activated carbon (commercial grade) was purchased from Biocat. Graphite (commercial grade) was purchased from Chenli. Copper (II) nitrate trihydrate ($Cu(NO_3)_2 \cdot 3H_2O$), Potassium permanganate ($KMnO_4$), *N,N′*-dimethylformamide (DMF) and Hydrochloric acid (HCl) were supplied from Carlo-Erba Reagents. Potassium hydroxide (KOH) was obtained from Kem Aus. Sulfuric acid (H_2SO_4) was purchased from QReC. Sodium nitrate ($NaNO_3$) was obtained from Univar. Hydrogen peroxide (H_2) was purchased from Chem-supply. Nitrogen gas (99.999% UHP) was supplied by S.I. Technology Co., Ltd. (Thailand).

2.2 Preparation of Cu_xO doped activated carbon

The apricot stones were washed, dried, and then sealed and carbonized at 400°C with a 10°C·min^{-1} heating rate for 1 h to form apricot stone coals. The coals (30.0 g) and KOH (2.5 M) were vigorously mixed at 80°C for 2 h and then allowed to cool to room temperature (RT). The treated coals were filtrated and then dried at 120°C for 12 h to eliminate humidity. After that, the coals were calcinated at 850°C with a 10°C·min^{-1} heating rate for 1 h under an N_2 atmosphere to obtain apricot stone activated carbon (AAC). Subsequently, 5 wt% of Cu was doped in AAC by the incipient wetness impregnation method using a copper nitrate solution, followed by heat treatment at 550°C with 5°C·min^{-1} heating rate for 2 h under N_2 gas flow to obtain Cu (5 wt%) doped AAC, denoted as *AAC-5Cu$_x$O*. Additionally, 5 wt% of Cu doped commercial activated carbon (CAC) was prepared using a similar method to obtain the Cu (5 wt%) doped CAC, denoted as *CAC-5Cu$_x$O*, as shown in Figure 2. The metal doping method and thermal treatment process followed the optimized condition of a previously published report [20].

2.3 Synthesis of CuO-doped reduced graphene oxide

Graphene oxide was prepared following Hummer's method [21]. Graphite sticks were pulverized into powder and then dried at 120°C in an oven overnight. Graphite powder (2.0 g) and $NaNO_3$ (2.0 g) were mixed with concentrated H_2SO_4 (100.0 mL) in a round bottom flask under vigorous stirring in an ice bath for 12 h. While maintaining vigorous agitation, $KMnO_4$ (10.0 g) and deionized (DI) water (20.0 mL) were added to the suspension and then continuously stirred for another 6 h. The ice bath was removed, and the suspension was allowed to regain RT. As the reaction progressed, the mixture was gradually added with DI water (180.0 mL) and refluxed at 90°C for 30 min. Finally, H_2O_2 (40.0 mL) and DI water (100.0 mL) were added, and a yellowish-brown solution of graphene oxide was obtained. The prepared GO solution was centrifuged to remove impurities by HCl (0.1 M) and neutralized by DI water. The GO was then dried at 60°C for 24 h. Subsequently, 5 wt% of Cu was impregnated in the dried form of graphitic oxide by copper nitrate solution, followed by heat treatment at 110°C for 12 h in air and calcination at 300°C with 5°C·min^{-1} heating rate for 1 h under N_2 atmosphere to obtain Cu doped (5 wt%) reduced graphene oxide, denoted as *rGO-5Cu$_x$O*, as shown in Figure 2. The thermal reduction process followed a previous report [22].

2.4 Synthesis of Cu_xO doped carbon nanofiber

Copper-doped carbon nanofiber (CNF) was fabricated by polymeric electrospinning followed by conventional heat treatment. As demonstrated in a previous report [22], PAN powder (8 wt%) was dissolved in dimethylformamide (DMF) under a magnetic stirrer for 12 h at RT. Copper nitrate (5 wt% calculated as base polymer matrix) was added to the prepared solution, with stirring at RT until a homogeneous solution was obtained. The polymeric solution precursor was electrospun into polymeric fibers through a stainless steel gauge needle connected to the anode of a direct current supply at a high voltage of 15 kV and flow rate of 0.05 mL·min^{-1}. An aluminum foil sheet covered a stainless steel roller as a collector with the distance between the needle tip and collector set at 15 cm. The process was carried out in the air at RT. Finally, the obtained as-spun fibers were transformed into carbon by thermal treatment. The as-spun fibers were stabilized at 260°C for 2 h with a heating rate of 1°C·min^{-1} followed by annealing at 900°C at 10°C·min^{-1} heating rate for 1 h under an N_2 atmosphere to obtain Cu (5 wt%) doped CNF, denoted as *CNF-5Cu$_x$O*, as shown in Figure 2.

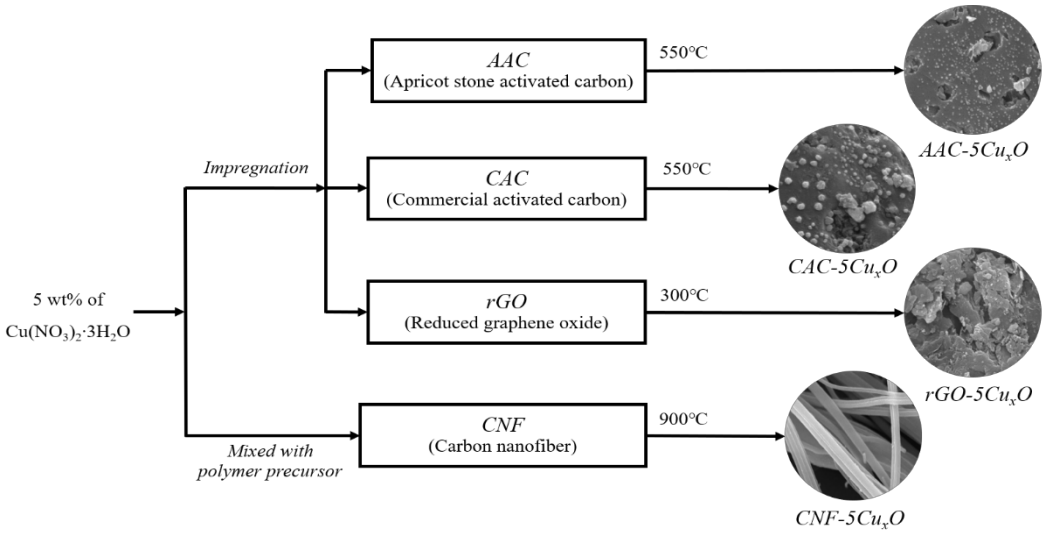

Figure 1. Experimental diagram of copper oxide doped different carbon substrates.

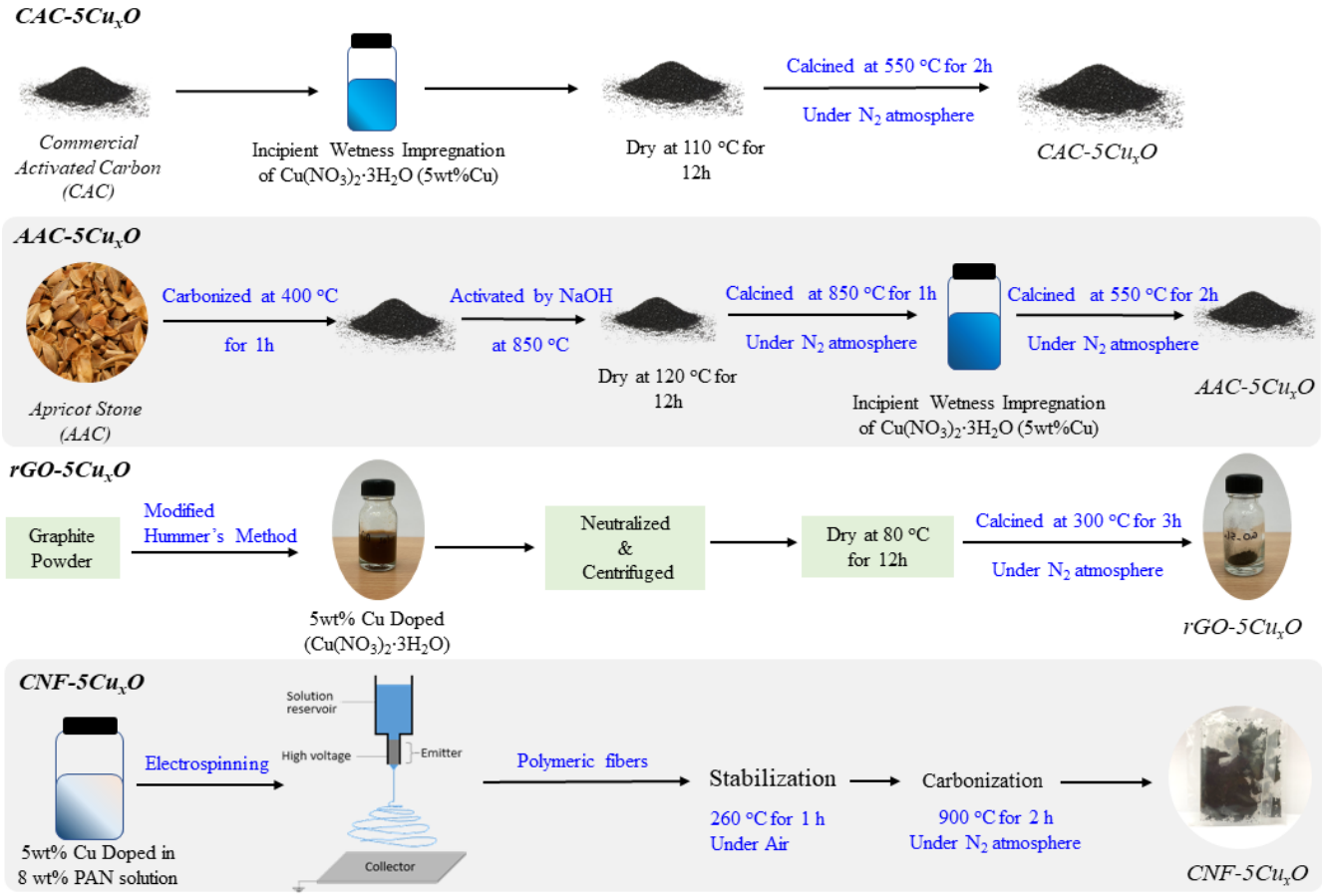

Figure 2. Steps in synthesis the doped-Cu samples.

2.5 Antimicrobial test

The antibacterial properties of the three Cu-doped carbon substrates were tested by the disc diffusion method to measure the inhibition zone of their activities against pathogens. Typical gram-positive and gram-negative bacteria such as *S. aureus* and *E. coli* were selected as modes, with an initial bacterial concentration of 1×10^8 CFU·mL^{-1}. The plates were sealed with parafilm and incubated at 37°C for 18 h before, and the distance (mm) of each inhibitory zone was measured. Clear zones around the samples were observed after 18 h of incubation. Ethyl alcohol (70%), sterilized NaCl solution (0.85%) and sterilized water were used as controls [23]. All measurements were conducted in triplicate, and the data were reported as mean ± standard deviation.

2.6 Spectroscopic measurement

The chemical functions of rGO and the as-spun fibers were analyzed by Fourier transform infrared spectroscopy (FTIR) using a Spectrum 100 (PerkinElmer, USA). Data were collected using an attenuated total reflection (ATR) technique connected to infrared spectroscopy with 16 scans/samples. The chemical components were examined by powder X-ray diffraction (XRD), model D8 advanced X-ray diffractometer (Bruker, USA) equipped with a Cu Kα sealed tube X-ray source (1.5418 Å). Data were collected in the range from 5.0° to 60.0° 2θ in steps of 0.02° with a scan speed of 0.5 sec/step. The physical morphology of the carbon fiber samples was detected by a Scanning electron microscope (SEM), model JSM-6610LV (JEOL, Japan).

3. Results and discussion

3.1 Chemical functions analysis

To confirm the existence of copper nitrate in the electrospun fibers and monitor the oxide formation over graphite structure, the chemical functions of the electrospun fibers, graphite, and rGO were characterized by infrared spectroscopy, with the spectra shown in Figure 3. The as-prepared Cu-doped PAN fibers (pink line) were compared with pure PAN fibers (blue line). Vibrational frequencies of the as-spun nanofibers are shown in the range from 3000 cm^{-1} to 400 cm^{-1}. Both PAN fibers showed clear characteristic signals, in agreement with the PAN spectrum at 2245 cm^{-1} and 1454 cm^{-1} of the C≡N group and C−H bending, respectively. The spectrum of Cu-PAN fibers included the characteristic vibration of PAN and also a strong absorption band at 1330 cm^{-1} assigned to O-H bending. The occurrence of OH bending resulted from water molecules in the lattice of the copper nitrate precursor, implying that copper was dispersed in the PAN fibers [24]. The spectrum of rGO showed broad signals of 1722 cm^{-1} and 1044 cm^{-1} assigned to C-O functional groups and C-O alkoxy groups, which corresponds to previous reports [25-27]. When compared to the graphite spectrum, these observed functional groups indicated that the graphite powder was successfully oxidized into rGO.

3.2 Chemical composition of particles

The phase composition of Cu in the three different carbon substrates was examined by XRD, with diffraction patterns presented in Figure 4. Diffraction peaks observed at 2θ values of 28.7°, 36.5°, and 42.5° corresponded to the (110), (111), and (200) planes, respectively. These reflections were similar to the characteristic diffraction peaks of the monoclinic phase of Cu_2O [28]. The CuO peaks observed at 2θ values of 32.7°, 35.5°, and 38.8° corresponded to the (110), (-111) and (111) planes, respectively [15]. Therefore, both copper oxide phase compositions were successfully formed on the different substrates. The characteristic pattern of each carbon substrate had 2θ values of 21° (CAC), 21° (rGO), and 22° (CNF) corresponding to copper oxides in contact with carbon substrates [29]. These reflection patterns confirmed that copper oxide particles were attached to the carbon surfaces.

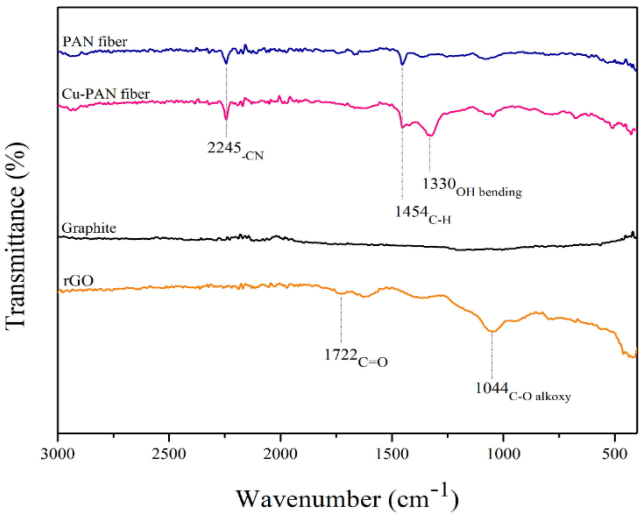

Figure 3. FTIR spectra of as-prepared fibers, graphite, and rGO.

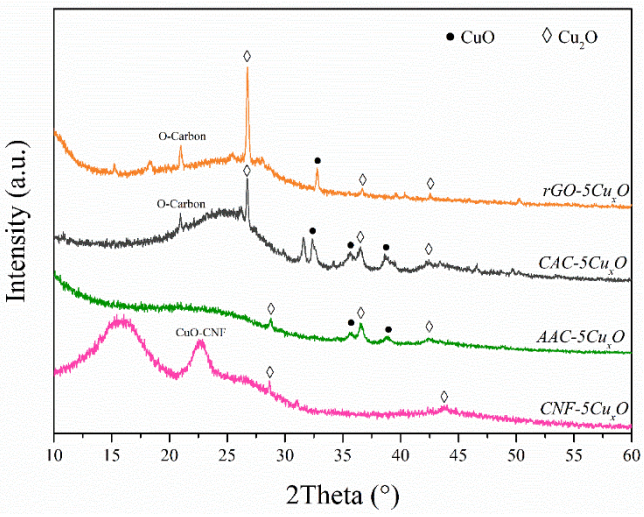

Figure 4. XRD pattens of CuO doped on different carbon substrates.

3.3 Morphology

Surface morphologies of the Cu_xO-doped activated carbon substrates were observed by SEM images, as presented in Figure 5. Interestingly, the *AAC-5Cu$_x$O* surface showed acceptable dispersion of Cu_xO-NPs with an average size of around 100 nm (43%), while the *CAC-5Cu$_x$O* sample had relatively fewer pores on the surface providing a larger size of Cu_xO-NPs at around 300 nm. Larger particle formation resulted from a relatively lower surface area or poor dispersion of Cu_xO-NPs. Additionally, the observed particle size distribution demonstrated that copper oxide formed the various particles size between 60 nm to 180 nm with the most population found at 100 nm about 43.0% for *AAC-5Cu$_x$O*. Besides, the size distribution for *CAC-5Cu$_x$O* gave Gaussian distribution of the particles size between 100 nm and 500 nm with a maximum count of about 63.5% for 300 nm. The Cu_xO-NPs on the AAC surface showed less aggregation because the small pores increased the specific surface area and reduced the size of the nanoparticles [30]. High surface area promotes the dispersion of nano-objects over carbon substrates [31].

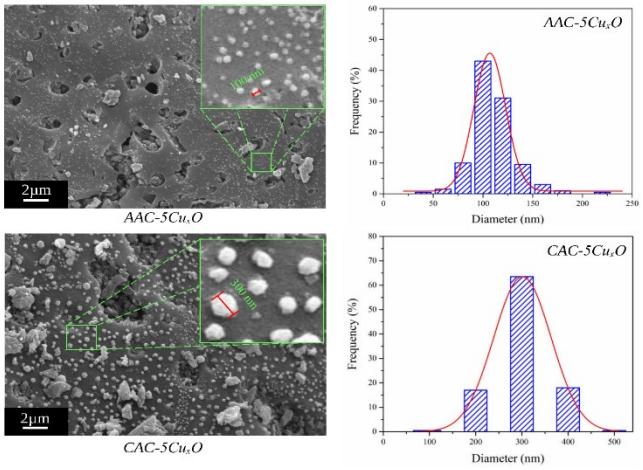

Figure 5. SEM images and particle size distribution for *AAC-5Cu$_x$O* and *CAC-5Cu$_x$O*

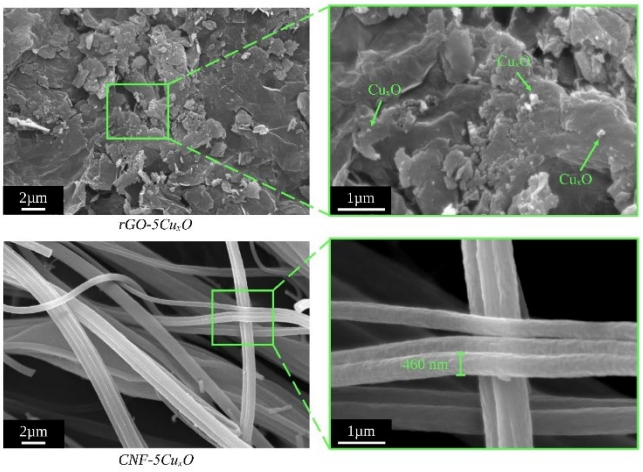

Figure 6. SEM images at low magnification (left) and high magnification for *rGO-5Cu$_x$O*, and *CNF-5Cu$_x$O*.

The surface morphology for *rGO-5Cu$_x$O* and *CNF-5Cu$_x$O* samples is shown in Figure 6. For *rGO-5Cu$_x$O*, although the oxide particles were poorly observed over the rGO surface, the XRD results confirmed the existence of CuO and Cu_2O in the rGO matrix. However, a tiny spherical shape with a diameter size of less than 100 nm was found over the rGO surface when zooming in at 20K-times magnification. This result implies that copper oxide particles can disperse over the rGO surface layer, whereas some particles might penetrate between the rGO layers. Furthermore, the rGO substrate not only prevented aggregation of the oxide particles but also reduced the particle size of copper oxide. For the *CNF-5Cu$_x$O* sample, the SEM image show uniform and smooth fiber with a diameter size of about 460 nm. The observation over the CNF surface found that copper oxide particles were not visible over the surface. However, the XRD results confirmed the existence of Cu_2O in the CNF matrix. Therefore, the Cu_2O particles may be packed inside the CNF matrix during thermal treatment at the carbonization step. Similar to the Cu-doped in the rGO substrate, the XRD pattern provided evidence that the Cu_2O was present in the CNF substrate. Therefore, the relatively high surface area of carbon substrate can be well dispersed and reduce the particle size of copper oxide.

3.4 Antimicrobial activity

The antimicrobial activity of the Cu$_x$O-NPs on various carbon substrates was tested against the pathogens *Staphylococcus aureus* and *Escherichia coli*. Figure 7 shows the clear zones of antibacterial activity of Cu$_x$O-doped carbon substrates. The larger size (mm) of the inhibition zone indicated high antibacterial activity (Table 1). Among carbon substrates, the *AAC-5Cu$_x$O* sample demonstrated excellent antimicrobial activity against *E. coli* with the largest clear zone (12.67 mm) and the smallest particles observed on the carbon surface, thereby enhancing antibacterial activity [32]. The occurrence of a clear zone may be due to the interruption of cell membranes by the Cu$_x$O-NPs, which correspond to previous reports [33]. The *AAC-5Cu$_x$O* offered high performance against negative bacteria but the clear zone against *S. aureus* did not appear. The less observed inhibition zone against *S. aureus* may result from the positive charge of copper ions having poor contact with the same positive charge of *S. aureus*'s cell membranes [34].

According to the *CAC-5Cu$_x$O* and *rGO-5Cu$_x$O* samples, a moderate inhibition zone against *E. coli* was found at around 8.67 mm and 9.67 mm, respectively, while the inhibition zone for both bacteria did not occur in the *CNF-5Cu$_x$O* sample. The moderate antimicrobial activity of *CAC-5Cu$_x$O* may be influenced by the larger particle size of the copper oxide nanoparticles. The large Cu$_x$O nanoparticle size has relatively low activity to inhibit bacteria growth [35]. Although the *rGO-5Cu$_x$O* sample provides a small copper oxide particle size of less than 100 nm, it offers moderate antimicrobial activity due to the tiny oxide particles penetrated between the rGO layers being in poor contact with the pathogen cells. Moreover, the *rGO-5Cu$_x$O* sample was stacked into a large and rigid rGO sheet, which may not release to liquid media. The absence of antimicrobial activity for the CNF substrate was because the Cu_2O-NPs were encapsulated inside the CNF matrix and not in contact with the pathogen cells. Although the nanostructure of carbon nanotube materials provided antimicrobial properties [17,36-37], this CNF sample not exhibiting the zone of inhibition may be due to the larger diameter size of carbon fiber. Samadian *et al*. [5] reported that the degree of genotoxicity for electro-spun CNFs derived from PAN followed by heat treatment may be less than that of traditional CNFs.

The antimicrobial activity of the synthesized samples is summarized in Figure 8. According to the *E. coli* inhibition zone, the copper oxide doped on AAC substrate can reduce the particle size of Cu$_x$O anchoring on carbon surface and efficiently inhibit the growth of *E. coli*. By contrast, the zone of inhibition against *S. aureus* was poorly observed because the concentration of Cu$_x$O-NPs was not suitable against *S. aureus* bacteria.

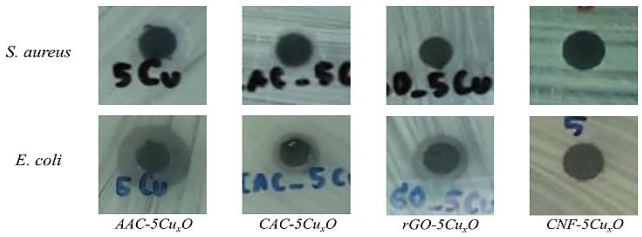

Figure 7. Zone of inhibition for Cu$_x$O-NPs doped different carbon substrates against *S. aureus* and *E. coli*.

Table 1. Three replicates test for antimicrobial performance of recently reported Cu_xO doped carbon substrates.

Samples	Clear Zone (mm)	
	S. aureus	*E. coli*
AAC	0	0
CAC	0	0
rGO	0	0
CNF	0	0
AAC-5Cu$_x$O	0	12.67±0.58
CAC-5Cu$_x$O	0	8.67±0.58
rGO-5Cu$_x$O	0	9.67±1.53
CNF-5Cu$_x$O	0	0

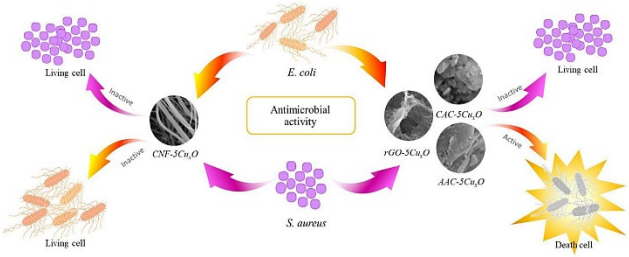

Figure 8. Antimicrobial activity of Cu_xO doped on various carbon substrates.

4. Conclusions

Cu_xO-NPs were successfully deposited on three different carbon substrates and demonstrated antimicrobial performance against *E. coli*, but not *S. aureus*. The *AAC-5Cu$_x$O* sample exhibited good antibacterial activity, while *CAC-5Cu$_x$O* and *rGO-5Cu$_x$O* samples exhibited moderate activity. The Cu_2O form in the CNF matrix had no clear zone because Cu_2O particles were packed inside the CNF matrix, while AAC material with tiny pores on the surface enhanced the formation of smaller particle-sized Cu_xO than the CAC substrate. Therefore, the antimicrobial activity of 5 wt% Cu_xO doped samples is effectively influenced by physical properties such as size, shape, surface area and position as well as the form of copper oxide. Furthermore, different Cu_xO-NPs sizes and morphologies are correlated with aspects of carbon substrates.

Acknowledgements

This study was supported by Thailand Science Research and Innovation Fundamental Fund (Project No. TUFF07/2564).

References

[1] R. Brown, G. Craun, A. Dufour, J. Eisenberg, J. Foran, C. Gauntt, C. Gerba, C. Haas, A. Highsmith, and R. Irbe, "A conceptual framework to assess the risks of human disease following exposure to pathogens," *Risk analysis,* vol. 16, pp. 841-848, 1996.

[2] O. E. Heuer, H. Kruse, K. Grave, P. Collignon, I. Karunasagar, and F. J. Angulo, "Human health consequences of use of antimicrobial agents in aquaculture," *Clinical Infectious Diseases,* vol. 49, pp. 1248-1253, 2009.

[3] K. Mortezaee, M. Najafi, H. Samadian, H. Barabadi, A. Azarnezhad, and A. Ahmad, "Redox Interactions and genotoxicity of metal-based nanoparticles: A comprehensive review," *Chemico-Biological Interactions*, vol. 312, p. 108814, 2019.

[4] H. Barabadi, H. Vahidi, K. D. Kamali, M. Rashedi, O. Hosseini, and M. Saravanan, "Emerging theranostic gold nanomaterials to combat colorectal cancer: A systematic review," *Journal of Cluster Science*, vol. 31, p. 651, 2020.

[5] H. Samadian, M. S. Salami, M. Jaymand, A. Azarnezhad, M. Najafi, H. Barabadi, and A. Ahmad, "Genotoxicity assessment of carbon-based nanomaterials; Have their unique physico-chemical properties made them double-edged swords?," *Mutation Research*, vol. 783, pp. 108296, 2020.

[6] H. Samadian, S. Zakariaee, M. Adabi, H. Mobasheri, M. Azami, and R. Faridi-Majidi, "Effective parameters on conductivity of mineralized carbon nanofibers: An investigation using artificial neural networks," *RSC Advances*, vol. 6, pp. 111908-111918, 2016.

[7] K. Gold, B. Slay, M. Knackstedt, and A. K. Gaharwar, "Anti-microbial activity of metal and metal-oxide based nanoparticles," *Advanced Therapeutics,* vol. 1, p. 1700033, 2018.

[8] S. M. Dizaj, F. Lotfipour, M. Barzegar-Jalali, M. H. Zarrintan, and K. Adibkia, "Antimicrobial activity of the metals and metal oxide nanoparticles," *Materials Science and Engineering,* vol. 44, pp. 278-284, 2014.

[9] J. Ramyadevi, K. Jeyasubramanian, A. Marikani, G. Rajakumar, and A. A. Rahuman, "Synthesis and antimicrobial activity of copper nanoparticles," *Materials letters,* vol. 71, pp. 114-116, 2012.

[10] M. F. Gutiérrez, P. Malaquias, V. Hass, T. P. Matos, L. Lourenço, A. Reis, A. D. Loguercio, and P. V. Farago, "The role of copper nanoparticles in an etch-and-rinse adhesive on antimicrobial activity, mechanical properties and the durability of resin- dentine interfaces," *Journal of Dentistry,* vol. 61, pp. 12-20, 2017.

[11] A. Čongrádyová, K. Jomová, L. Kucková, J. Kožíšek, J. Moncoľ, and M. Valko, "Antimicrobial activity of copper (II) complexes," *Journal of Microbiology, Biotechnology and Food Sciences,* vol. 2021, pp. 67-70, 2021.

[12] S. E.-D. Hassan, S. S. Salem, A. Fouda, M. A. Awad, M. S. El-Gamal, and A. M. Abdo, "New approach for antimicrobial activity and bio-control of various pathogens by biosynthesized copper nanoparticles using endophytic actinomycetes," *Journal of Radiation Research and Applied Sciences,* vol. 11, pp. 262-270, 2018.

[13] M. S. Usman, M. E. El-Zowalaty, K. Shameli, N. Zainuddin, M. Salama, and N. A. Ibrahim, "Synthesis, characterization, and antimicrobial properties of copper nanoparticles," *International journal of nanomedicine,* vol. 8, pp. 4467, 2013.

[14] G. Ren, D. Hu, E. W. Cheng, M. A. Vargas-Reus, P. Reip, and R. P. Allaker, "Characterisation of copper oxide nano-particles for antimicrobial applications," *International journal of antimicrobial agents,* vol. 33, pp. 587-590, 2009.

[15] S. Singh, M. Ashfaq, R. K. Singh, H. C. Joshi, A. Srivastava, A. Sharma, and N. Verma, "Preparation of surfactant-mediated silver and copper nanoparticles dispersed in hierarchical carbon micro-nanofibers for antibacterial applications," *New biotechnology,* vol. 30, pp. 656-665, 2013.

[16] R. Mohan, A. Shanmugharaj, and R. Sung Hun, "An efficient growth of silver and copper nanoparticles on multiwalled carbon nanotube with enhanced antimicrobial activity," *Journal of Biomedical Materials Research Part B: Applied Biomaterials,* vol. 96, pp. 119-126, 2011.

[17] S. Mohammed, K. Khashan, M. Jabir, F. Abdulameer, G. Sulaiman, M. Al-Omar, H. Mohammed, A. Hadi, and R. Khan, "Copper oxide nanoparticle-decorated carbon nanoparticle composite colloidal preparation through laser ablation for antimicrobial and antiproliferative actions against breast cancer cell line, MCF-7," *BioMed Research International,* vol. 2022, pp. 1-13, 2022.

[18] J. R. Nascimento, M. R. D'Oliveira, A. G. Veiga, C. A. Chagas, and M. Schmal, "Synthesis of reduced graphene oxide as a support for nano copper and palladium/copper catalysts for selective NO reduction by CO," *ACS Omega,* vol. 5, pp. 25568-25581, 2020.

[19] W. Shao, S. Wang, J. Wu, M. Huang, H. Liu, and H. Min, "Synthesis and antimicrobial activity of copper nanoparticle loaded regenerated bacterial cellulose membranes," *RSC advances,* vol. 6, pp. 65879-65884, 2016.

[20] A. Abdedayem, M. Guiza, and A. Ouederni, "Copper supported on porous activated carbon obtained by wetness impregnation: Effect of preparation conditions on the ozonation catalyst's characteristics," *Comptes Rendus Chimie,* vol. 18, pp. 100-109, 2015.

[21] W. S. Hummers, and R. E. Offeman, "Preparation of graphitic oxide," *Journal of the American Chemical Society,* vol. 80, pp. 1339-1339, 1958.

[22] S. Thiangviriya, and R. Utke, "$LiBH_4$ nanoconfined in activated carbon nanofiber for reversible hydrogen storage," *International Journal of Hydrogen Energy,* vol. 40, pp. 4167-4174, 2015.

[23] C. Das, S. Sen, T. Singh, T. Ghosh, S. S. Paul, T. W. Kim, S. Jeon, D. K. Maiti, J. Im, and G. Biswas, "Green synthesis, characterization and application of natural product coated magnetite nanoparticles for wastewater treatment," *Nanomaterials,* vol. 10, pp. 1615, 2020.

[24] C. Daniel, Y. Schuurman, and D. Farrusseng, "Surface effect of nano-sized cerium-zirconium oxides for the catalytic conversion of methanol and CO_2 into dimethyl carbonate," *Journal of Catalysis,* vol. 394, pp. 486-494, 2021.

[25] J. R. Anasdass, P. Kannaiyan, R. Raghavachary, S. C. B. Gopinath, and Y. Chen, "Palladium nanoparticle-decorated reduced graphene oxide sheets synthesized using Ficus carica fruit extract: A catalyst for Suzuki cross-coupling reactions," *PLOS ONE,* vol. 13, pp. e0193281, 2018.

[26] B. D. Ossonon, and D. Bélanger, "Synthesis and characterization of sulfophenyl-functionalized reduced graphene oxide sheets," *RSC Advances,* vol. 7, pp. 27224-27234, 2017.

[27] M. Ruidíaz-Martínez, M. A. Álvarez, M. V. López-Ramón, G. Cruz-Quesada, J. Rivera-Utrilla, and M. Sánchez-Polo, "Hydro-thermal synthesis of rGO-TiO_2 composites as high-performance UV photocatalysts for ethylparaben degradation," *Catalysts,* vol. 10, pp. 520, 2020.

[28] Q. He, Y. Tian, Y. Wu, J. Liu, G. Li, P. Deng, and D. Chen, "Electrochemical sensor for rapid and sensitive detection of tryptophan by a Cu_2O nanoparticles-coated reduced graphene oxide nanocomposite," *Biomolecules,* vol. 9, pp. 176, 2019.

[29] R. Siburian, H. Sihotang, S. L. Raja, M. Supeno, and C. Simanjuntak, "New route to synthesize of graphene nano sheets," *Oriental Journal of Chemistry,* vol. 34, pp. 182, 2018.

[30] C.-S. Yang, Z. Sun, C.-H. Cui, C. Yang, and T. Zhang, "Metal nano-drills directionally regulate pore structure in carbon," *Carbon,* vol. 175, pp. 60-68, 2021.

[31] H. Fei, Z. Peng, L. Li, Y. Yang, W. Lu, E. L. Samuel, X. Fan, and J. M. Tour, "Preparation of carbon-coated iron oxide nanoparticles dispersed on graphene sheets and applications as advanced anode materials for lithium-ion batteries," *Nano Research,* vol. 7, pp. 502-510, 2014.

[32] A. Azam, A. S. Ahmed, M. Oves, M. Khana and A. Memic, "Size-dependent antimicrobial properties of CuO nanoparticles against Gram-positive and-negative bacterial strains," *International journal of nanomedicine,* vol. 7, pp. 3527, 2012.

[33] P. Bhavyasree and T. Xavier, "Green synthesis of copper oxide/carbon nanocomposites using the leaf extract of *Adhatoda vasica Nees*, their characterization and antimicrobial activity," *Heliyon,* vol. 6, p. e03323, 2020.

[34] M. Hajipour, K. Fromm, A. A. Ashkarran, D. J. de Aberasturi, I. Larramendi, T. Rojo, V. Serpooshan, W. Parak, and M. Mahmoudi, "Antibacterial properties of nanoparticles," *Trends in Biotechnology,* vol. 30, pp. 499-511, 2012.

[35] A. Azam, "Size-dependent antimicrobial properties of CuO nanoparticles against Gram-positive and -negative bacterial strains," *International Journal of Nanomedicine,* pp. 3527, 2012.

[36] M. Al-Omar, M. Jabir, E. Karsh, R. Kadhim, G. Sulaiman, Z. Taqi, K. Khashan, H. Mohammed, R. Khan and S. Mohammed, "Gold nanoparticles and graphene oxide flakes enhance cancer cells' phagocytosis through granzyme-perforin-dependent biomechanism," *Nanomaterials,* vol. 11, pp. 1382, 2021.

[37] H. Hamouda, H. Abdel-Ghafar, and M. Mahmoud, "Multi-walled carbon nanotubes decorated with silver nanoparticles for antimicrobial applications," *Journal of Environmental Chemical Engineering,* vol. 9, pp. 105034, 2021.